



Computational screening of chemical constituents derived from berry fruits as allosteric caspase-3/-7 inhibitors

Waseem Ahmad Ansari¹ · Mohsin Ali Khan² · S. M. Mahfooz Hasan² · Zainab Siddiqui² · Saheem Ahmad³ · Mohd Shahnawaz Khan⁴ · Mohammad Faheem Khan^{1,5}

Received: 11 May 2024 / Accepted: 23 August 2024
© King Abdulaziz City for Science and Technology 2024

Abstract

With the aim of finding the plant-derived allosteric inhibitors of caspase-3/-7, we conducted computational investigations of bioactive compounds present in various berry fruits. In a molecular docking study, perulactone demonstrated excellent binding affinity scores of -12.1 kcal/mol and -9.1 kcal/mol for caspase 7 and 3, respectively, whereas FDA-approved allosteric inhibitors (DICA and FICA) were found to show lower docking scores (-5.6 and -6.1 kcal/mol) against caspase 7 while (-5.0 and -5.1 kcal/mol) for caspase 3, respectively. MD simulations were used to validate the binding stability of perulactone in the active sites of caspase-7/-3, and the results showed outstanding stability with lower ligand RMSDs of 1.270 – 3.088 Å and 2.426 – 9.850 Å against the targeted receptor. Furthermore, we performed MMGBSA free binding energy, where the perulactone values of ΔG_{Bind} were determined to be -63.98 kcal/mol and -66.32 kcal/mol for both receptors (3IBF and 1NME), which are significantly better than the -45.16 kcal/mol and -39.51 kcal/mol for DICA as well as -26.37 kcal/mol and -15.50 kcal/mol for FICA, respectively. The drug resemblance of perulactone was effectively evaluated by ADMET. Thus, our findings indicated that perulactone could be an orally administered therapeutic candidate for regulating apoptosis in a variety of disorders. However, there may be an urgent need to study using in vitro and in vivo experiments.

Keywords Allosteric site · Molecular docking · Molecular dynamic simulation · Berry fruits · MMGBSA calculation

Introduction

Apoptosis, also known as programmed cell death, is an essential component of cellular homeostasis that is utilized to destroy undesirable cells or debris that has accumulated

beyond repair during biochemical activities (Chaudhry et al. 2022). Apoptosis cell death is characterized by cell shrinkage, membrane blebbing, condensation of chromatin fibers, as well as DNA fragmentation (Green and Llambi 2015). Because of the killing of undesirable cells, apoptosis is most crucial for maintaining general cellular structures and functions in multicellular organisms. Stopping apoptosis can result in uncontrolled cell division, which leads to the development of several diseases such as inflammation, atherosclerosis, autoimmune, neurodegenerative and cancer (Loftus et al. 2022). Two pathways, including the intrinsic pathway that leads to mitochondrial-initiated events and the extrinsic pathway that is initiated by death receptors (Xu and Shi 2007) can trigger apoptosis. In the intrinsic pathway, loss in the transmembrane potential of mitochondria releases pro-apoptotic proteins from the inner membrane into the space of the cytosol. As a result, it triggers the activation of caspase proteins, which leads to a misbalance of the apoptosis process (Ouyang et al. 2012). Caspases, regulators of apoptosis, are cysteine proteases that cleave their substrate at aspartate residues. These proteases

✉ Mohammad Faheem Khan
faheemkhan35@gmail.com

¹ Department of Biotechnology, Era's Lucknow Medical College & Hospital, Era University, Sarfarazganj, Hardoi Road, Lucknow 226003, India

² Center for Disease Mapping and Therapeutic Research, Era's Lucknow Medical College & Hospital, Era University, Sarfarazganj, Hardoi Road, Lucknow 226003, India

³ Department of Medical Laboratory Science, College of Applied Medical Sciences, University of Hail, 2440 Hail, Saudi Arabia

⁴ Department of Biochemistry, College of Sciences, King Saud University, 12371 Riyadh, Saudi Arabia

⁵ Department of Chemistry, Era University, Sarfarazganj, Hardoi Road, Lucknow 226003, India

involve initiator caspases (caspase-2, -8, -9, -10, -11, and -12) and downstream effector caspases (caspase-3, -6, and -7), which are closely coupled to pro-apoptotic signals (Parrish and Freel 2013). Several pro-apoptotic proteins, such as cytochrome c, endonuclease G (EndoG), the second mitochondria-derived activator of caspase/direct inhibitor of apoptosis-binding protein with low pI (Smac/DIABLO), and others, are found in the inner space of the mitochondrial membrane and cause apoptosis when disrupted. The process is known as mitochondrial outer membrane permeabilization (MOMP), which occurs when mitochondrial inner transmembrane potential is lost, resulting in the synthesis of ATP and reactive oxygen species (ROS) and thus triggering cell death (O'Brien and Kirby 2008). Additionally, the protein Apaf-1 and cytochrome c link together to activate caspase-9, which in turn activates caspase-3/-7. During apoptosis, this complete cascade causes membrane blebbing, DNA fragmentation, and cell shrinkage (Shi 2002; Lakhani et al. 2006). According to Matthew Brentnall et al., caspase-3 prevented ROS formation, but caspase-7 has been linked to apoptotic cell detachment, resulting in effective cell death and protein cleavage (Brentnall et al. 2013). The catalytic cysteine residue in the active sites of caspase-3/-7 is identical, and they both cleave the same substrates with comparable efficiency (Kuribayashi et al. 2006). Conversely, both caspases show a high degree of specificity due to selective cleavage at the aspartic acid residue. This specificity relies on a concept of conformational selection, which binds the molecule preferentially in the stabilized site of the protein in a particular conformation while maintaining the equilibrium of numerous conformations (Laskowski et al. 2009). Furthermore, conformational selection can occur when a molecule binds to an orthosteric or allosteric site. When an endogenous ligand binds to an orthosteric site, a modulator molecule can bind to a topographically distinct allosteric site, causing a shift in the equilibrium between protein states and, as a result, an increase or decrease in agonistic action. On the other hand, targeting the ligand at the allosteric sites keeps the protein dynamic in balance, which is why they respond specifically to drug molecules (Conn et al. 2009). Considering the importance of the allostery concept, drug design may benefit from modifying allosteric responses. Allosteric medicines have the potential to display enhanced target selectivity, reduced side effects, and decreased drug resistance by specifically targeting several locations on a single protein (Häcker et al. 2011). As shown in the literature, allosteric inhibition of caspase-3/-7 could serve as a possible therapeutic target to halt apoptosis-based disorders such as cancer, Alzheimer's, Parkinson's, cardiac arrest, ischemic strokes, and so on (Kesavardhana et al. 2020). During some decades, several caspase inhibitors targeting binding sites or catalytic pockets have been explored, but they have limited efficacies due to extensive competition between caspases

and their indigenous substrates (Becker et al. 2004). Jeanne A. Hardy et al. uncovered new allosteric sites at the dimer interface of caspase-3/-7 enzymes. They screened numerous compounds having thiol linkage against allosteric sites of caspase-3/-7 and found that two molecules, namely 2-(2,4-Dichlorophenoxy)-*N*-(2-mercapto-ethyl)-acetamide (DICA) and 5-Fluoro-1*H*-indole-2-carboxylic acid (2-mercapto-ethyl)-amide (FICA), inhibit the peptide binding via the formation of disulfide bridges with cysteine residues, Cys264 in caspase-3 and Cys290 in caspase-7, in the central cavity presented at the dimer interface. The binding of both molecules at allosteric sites disturbs the orthodox binding, which results in the inactivation of caspase-3/-7. That's why these molecules act as allosteric inhibitors (Hardy et al. 2004). Previous investigations (in vitro and in vivo) have shown that several drugs, including some FDA-approved medications, had caspase inhibitory action (MacKenzie et al. 2010). Deepak et al. found that four compounds, diflunisal, flubendazole, fenoprofen, and pranoprofen, reduce caspase-3 activity in a recombinant caspase-3 enzyme assay. In this approach, every compound had significant IC₅₀ values ranging from 10.37 ± 0.5 to 54.32 ± 0.6 mM (Krishna Deepak et al. 2018). Furthermore, Lee et al. revealed isatin sulphonamide and 5-dialkylaminosulfonylisatins as non-peptide caspase-3/-7 protein inhibitors that reduce apoptosis in mouse bone marrow neutrophils, Jurkat T cells, and human chondrocytes. Interestingly, 5-dialkylaminosulfonylisatins binds to the S2 subsite of caspases 3/-7, which contains Tyr204, Trp206, and Phe256 amino acid residues, whereas isatin sulphonamide binds to the S2 subsite but not to the aspartic acid-binding pocket S1 (Lee et al. 2000, 2001).

Despite the presence of synthetic allosteric caspase inhibitors, many bioactive substances derived from medicinal plants, referred to as plant-derived compounds, have the ability to regulate apoptosis through caspase-dependent or independent processes (Rahman et al. 2021). Except medicinal plants, functional foods have gained a lot of attention as nutraceutical products because of their health benefits due to the presence of bioactive compounds in addition to nutrients like carbohydrates, amino acids, peptides, dietary fibers, vitamins, minerals and microelements (AlAli et al. 2021). Although there are thousands of plant-derived compounds with various pharmacological functions, herein, we will not detail them; instead, we will focus on berry fruits. Several studies revealed that berry fruits have health-improving effects and prevent chronic diseases as they are rich in nutrients and bioactive compounds (Golovinskaia and Wang 2021). Some species of berries, such as blackberries, blueberries, blackcurrants, cranberries, raspberries, and strawberries are good sources of polyphenols including flavonols, flavanols, ellagitannins, hydrolysable tannins, non-hydrolysable tannins, proanthocyanidins, anthocyanins and stilbenes (Nile and Park 2014). These bioactive compounds

have been found to show their antioxidant, anti-inflammatory, antidiabetic, antimicrobial, neuroprotective and cardio protective effects. Several in-vitro and in-vivo studies revealed that berry fruits have excellent antioxidant and anti-aging properties due to the presence of a high content of polyphenols, contributing to the organoleptic qualities of fruits (Bader UI Ain et al. 2022; Baby et al. 2017). As per the in-vitro study, six berries (blackberry, blueberry, raspberry, black raspberry, cranberry and strawberry) and their polyphenol compounds showed the anticancer effect by stimulating apoptosis of the COX-2 enzyme as well as inhibiting cell proliferations in HT-29/HCT116 colon cancer cells (Seeram et al. 2006). Cyanidin-3-glycoside, an anthocyanin of black raspberry, inhibited the oxidative DNA damage in human colon epithelial cells whereas inhibited the apoptosis and G1 phase of the cell population in cultured Caco-2, respectively (Duthie et al. 2004; Elisia and Kitts 2008). In some studies, phenolics and flavonoids rich fractions of cranberry as well as extracts of chokeberry and bilberry inhibited cell proliferation with progressive cell-cycle arresting that leads to apoptosis in HT-29 line colon cells (Ferguson et al. 2004; Zhao et al. 2004). Some lyophilized extracts of strawberries had been found to reduce tumor incidence via inhibiting pro-inflammatory mediators (TNF- α , IL-1 β , IL-6, COX-2, and iNOS), suppressing nitrosamine stress, and lowering down the overexpression of PI3-K, Akt, ERK, and NF- κ B cell signaling in the AOM/DSS mouse model (Shi et al. 2015). Regulating of cell cycle and apoptosis signaling are shown by ellagitannins (ellagic acid, urolithin A, urolithin B, and ellagic acid), cyanidin chloride, cyanidin-3-*O*-glucopyranoside and enterolactone in different cancer cell lines (in-vitro) as well as in rat models (in-vivo) as displayed by studies (Cho et al. 2015; Renis et al. 2008; Danbara et al. 2004). Apart from their pharmacological actions, numerous studies have demonstrated that the flavonoids, polyphenols, and withanolides (e.g., perulactones) derived from berry fruits reduce caspase activity via activating caspase enzyme activity, which in turn cleaves the pro-caspase into the active form. (Chien et al. 2009; Shen et al. 2003; Wang et al. 1999; Henrich et al. 2015). Myricetin suppressed caspase-3 activity (IC₅₀ 10.2 mM) in rat neural cell cultures, according to research by Shimmyo et al. By using the docking method, they investigated the chemical interaction in which the hydroxyl group on the myricetin B-ring interacted with Glu 123 and the ether oxygen bonded to the Arg 207 amino acid residues of the caspase-3 active site (Shimmyo et al. 2008). Ahmad Abdullah et al. demonstrated an in vitro assay in which kaempferol interacts with the caspase-3 enzyme at allosteric regions and inhibits it via a competitive mechanism. By molecular docking, kaempferol showed hydrophobic interactions and H-bonding interactions with the Cys 290 residue and the Val 292 and Met294 residues of caspase-7, while the Arg 164, Tyr 197, Glu 124, Arg 164, Thr 140,

Tyr 195, Val 266, Lys 137, Leu 136, Pro 201, and Gly 125 residues of caspase-3 showed hydrophobic interactions and H-bonding interactions (Abdullah and Ravanan 2018). Nevertheless, kaempferol may block caspase 7 in conjunction with other inhibitors to partially reverse apoptosis, suggesting that kaempferol can induce apoptosis through either an independent or caspase-dependent mechanism (Dang et al. 2015). Furthermore, it was shown that withanolides, like withaferin A, might control apoptosis in different colorectal cancer cell lines by cleaving caspase-3 and reducing anti-apoptotic proteins (Jung et al. 2022). Withaferin A demonstrated molecular interactions via the BIR domain with the apoptotic protein inhibitor in a docking study, which subsequently inhibited caspase-3/-7 (Wadegaonkar and Wadegaonkar 2012). Withanone also bound to the BIR domain of the apoptotic protein Survivin, and through this interaction, the two worked together. As a result, caspases-3/-7 are inhibited, which causes them to undergo apoptosis (Wadegaonkar and Wadegaonkar 2013).

The combined results of the aforementioned studies indicate that a number of flavonoids and withanolides can inhibit apoptotic proteins, such as caspases like caspase-3/-7. However, no information has been provided concerning the molecular mechanism underlying the inhibition of these compounds' allosteric caspases, which determines how they interact and cleave them. Motivated by this, we propose here that plant-derived compounds, particularly flavonoids and/or polyphenols, as well as withanolides, may offer a promising platform for the development of caspase inhibitors for the treatment of diseases associated with apoptosis. We thus tried to find the best allosteric inhibitor among the one hundred (100) compounds of berry fruits at their allosteric sites of caspase-3/-7 that are executioner proteins in apoptosis pathways. Our findings may help numerous researchers and scientists to build and identify therapeutic leads of plant origin against allosteric regions of caspase-3/-7 proteins.

Methodology

Selection of compounds for ADME screening

ADMET such as absorption, distribution, metabolism, excretion, and toxicity is used to screen the drug leads for their suitability via oral administration. We have prepared a library of 100 compounds from berry fruits premised on their pharmacological activities, especially anticancer activity from the previous literature investigations and then screened them for pharmacokinetics (ADMET) properties using an in silico approach with the help of the QikProp v6.8 module of Schrödinger 2020-4 LCC, New York, USA. All the selected compounds were examined for drug-like characteristics based on Lipinski's rule of five (Ro5) such

as molecular weight (≤ 500), hydrogen bond donor (≤ 5), hydrogen bond acceptor (≤ 10), and lipophilicity (≤ 5). Furthermore, pharmacokinetic parameters such as solubility, blood–brain barrier, human serum albumin, and oral absorption in humans were also determined (Teli et al. 2021). Furthermore, we employed Osiris Property Explorer software and ProTox 3.0 server to screen the toxicity characteristics, such as mutagenic, tumorigenic, irritating, and reproductive effects for all the compounds (<https://tox.charite.de/protox3/>).

Preparation of ligands and receptors

Amongst the selected compounds, we found only **1–20** compounds by displaying drug-like or drug-ability properties

with a full fill of Ro5. Thus, we took **1–20** compounds (Fig. 1) for further in-silico study. The three-dimensional (3D) structures of all compounds, along with the reference drugs, namely 2-(2,4-Dichlorophenoxy)-*N*-(2-mercaptoethyl)-acetamide (DICA) and 5-Fluoro-1*H*-indole-2-carboxylic acid (2-mercapto-ethyl)-amide (FICA), were obtained from PubChem (<https://pubchem.ncbi.nlm.nih.gov/>). The geometries of chemical structures were cleaned and optimized using the Merck molecular force field (MMFF) visualizer in Biovia Discovery Studio 3.0, then saved in.pdb format. The AutoDock4 software was also used to specify the detecting root, number of torsions, and aromaticity criteria (Khan et al. 2021). The three-dimensional crystallographic structures of caspase-3 (PDB ID:1NME) and caspase-7 (PDB ID:3IBF) receptors, with resolutions of 2.50 Å and

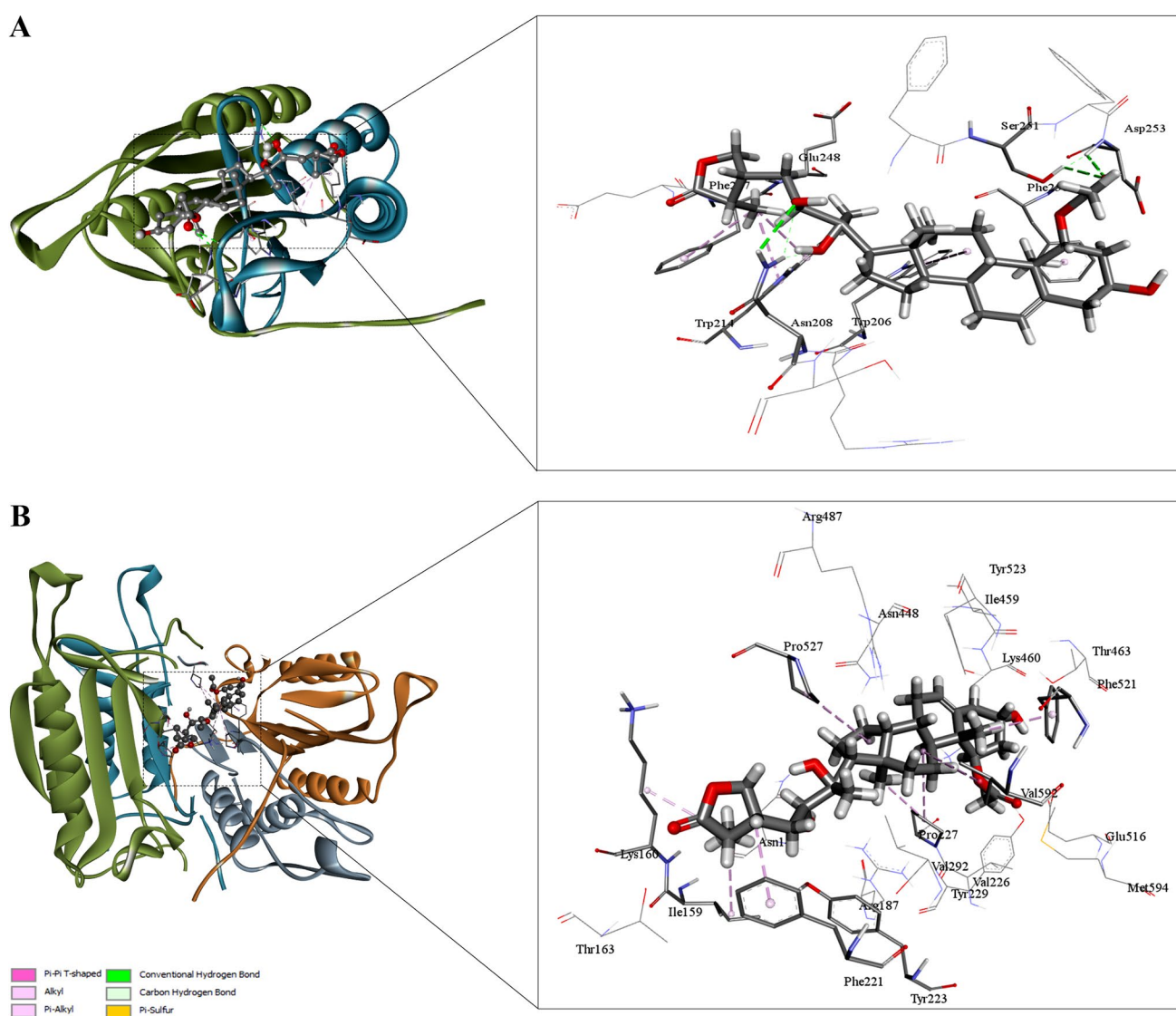


Fig. 1 The molecular docking poses **A** molecular interactions of perulactone with caspase 3 (PDB:1NME) protein, and **B** molecular interactions of perulactone with caspase-7 (PDB:3IBF) protein

1.60 Å (Erlanson et al. 2003; Agniswamy et al. 2009) were obtained from the RCSB Protein Data Bank (<https://www.rcsb.org/>). The Biovia Discovery Studio 3.0 visualizer was used to remove the water molecules and heteroatoms from the target protein structures before adding missing hydrogen atoms. To screen the interactions between receptor and ligand, the define site module of the Biovia Discovery Studio 3.0 visualizer was used to estimate the binding site coordinate of the targeted protein receptor. Furthermore, using the AutoDock4 software, polar hydrogen atoms and Kollman charges were used to prepare receptors for molecule docking (Tallei et al. 2020).

Molecular docking

The molecular docking approaches can be used to predict the ligand-receptor binding affinities. To explore the allosteric sites of 1NME and 3IBF targets against the best 1–20 compounds, the AutoDock Vina 1.1.2 software (developed by Dr. Oleg Trott, Scripps Research Institute) was used to perform receptor-oriented flexible docking. The grid box of $50 \times 50 \times 50 \text{ \AA}^3$ dimensions was optimised over the receptor binding site for molecular docking using $X = -3.704$, $Y = 13.032$, $Z = 4.398$ and $X = 41.857$, $Y = 95.643$, $Z = 24.016$ coordinates. The selected compounds were treated as flexible ligands, which mimic the binding with proteins in real system during docking. The final position was visualised using the Biovia Discovery Studio 3.0 visualizer after docking which is based on the lowest binding affinity (Khan et al. 2021; Singh and Purohit 2023; Singh et al. 2024). Herein, we reported the best docking scores in triplicate runs for each of compounds (1–20) against both the targets 1NME and 3IBF.

Molecular dynamic simulation

The study of molecular dynamic (MD) simulations is employed to better understand the deep insights of molecular interactions in between ligand–protein complexes. The ligand–protein complexes were created in the TIP3P (Transferable Intermolecular Potential with 3 Points) water system for MD simulation, and four Na^+ and five Cl^- ions were added to neutralize the entire system of two complexes, such as perulactone-3IBF and perulactone-1NME complexes. The ligand–protein complexes were encased in an orthorhombic box shape with $10 \text{ \AA} \times 10 \text{ \AA} \times 10 \text{ \AA}$ dimensions and minimized using the system builder module (Desmond Schrödinger 2020-4 LCC, New York, USA) and the OPLS_2005 (Optimised Potentials for Liquid Simulations) force field. Furthermore, the ligand–protein system as a whole was loaded from the workspace, and the time was set to 100 ns to estimate the complex's stability in the simulated biological system. Prior to the MD simulation,

the NPT thermodynamic parameter with 1.0 bar pressure at 300 K temperature was implemented. Furthermore, the RESPA (Reversible Reference System Propagator Algorithm) was used to calculate the time steps for the near and far-bonded (2–6 fs). The partial mesh was maintained using the Nose–Hoover chain thermostat and Martyna-Tobias-Klein barostat procedures. The electrostatic interaction between atoms was quantified using the Ewald method with a Coulombic radius cutoff of 9.0. After the MD simulations were completed, the energy was measured every 100 ps and the trajectory was analyzed using the SID (Simulation Interaction Diagram) panel (Khan et al. 2022a, b; Sheikh et al. 2023a, b; Kumar et al. 2023).

Prime MMGBSA calculations

Following MD simulation, the free binding energy of the docked complexes perulactone-1NME and perulactone-3IBF was validated using the prime module of the Molecular Mechanics-Generalized Born Surface Area (MMGBSA) module of Schrödinger 2020-4 LCC, New York, USA. The complexes were produced using the implicit VSGB (Variable Dielectric Generalized Born) solvation condition and then reduced using the OPLS_5 force field. The MMGBSA binding free energy of complexes was then computed using the thermal_mmgsa.py python program (Alghamdi et al. 2023; Khan et al. 2022a, b). The Gibbs-free energy, coulombic energy, generalized solvation energy, and van der Waal energy were calculated using the equation below:

$$\Delta G_{\text{binding}} = \Delta E_{\text{MM}} + \Delta G_{\text{solvent}} + \Delta G_{\text{SA}} \quad (1)$$

where $\Delta G_{\text{binding}}$ = Binding free energy; ΔE_{MM} = difference between ligand–protein complex energy and total energy of ligand and receptor; $\Delta G_{\text{solvent}}$ = difference between of solvation energy of ligand–protein complex and total solvation energy of ligand and receptor; ΔG_{SA} = difference between the surface area energy of ligand and receptor.

Result and discussion

Assessment of ADMET properties

The drug-abilities or drug-like properties of 100 compounds of berry fruits were evaluated using ADMET analysis to validate their necessary properties in Lipinski's rule of five (Ro5) for oral bioavailability. If any compound shows either zero or less than one violation, then it is considered an oral drug lead. Thus, it can be validated that a molecule can be submitted for its molecular docking study. Among the 100 compounds, only twenty compounds (1–20) passed out through the screening test of the Ro5 rule. A literature

survey also reveals that these compounds have various pharmacological activities like anticancer, anti-inflammatory, and antioxidant, but no study was reported at allosteric sites that inhibit the apoptosis pathway. In the present study, we obtained the perulactone as the best compound with good agreement with the Ro5 rule, including molecular weight (518.6), hydrogen bond donors (03), hydrogen bond acceptors (09), and lipophilicity (3.76). Moreover, we also predicted the pharmacokinetic properties of perulactone such as -5.78 mol/dm^3 aqueous solubility (standard range -6.5 to 0.5 mol/dm^3), -1.73 blood-brain barrier (standard range -3.0 to 1.2), 0.68 human serum albumin interaction (standard range -1.5 to 1.5), and high human oral absorptions (standard range 1 = low, 2 = moderate, 3 = high) respectively. Therefore, the perulactone demonstrated outstanding pharmacological activity, a drug-like candidate, and did not have any toxicity including mutagenic, tumorigenic, irritating, or reproductive effects. It also followed the recommended range of parameters of ADMET characteristics (Mohan et al. 2021). For all the compounds (1–20), ADME characteristics are displayed in Table 1 whereas Table 2 shows the toxicity profiles.

Molecular docking analysis

To filter the small molecule as a drug-like candidate from the chemical structure library, structure-based study is an extremely vital strategy, where molecular docking

investigations fit well in the area of ligand-receptor interactions. After screening the ADMET test, we performed a molecular docking study to explore the molecular interactions of compounds (1–20) within the allosteric sites of caspase-3 (1NME) and caspase-7 (3IBF) receptors. In this study, as a consequence of hydrogen bonds, hydrophobic interactions, and involved amino acids, docking scores (binding energy) were noted in kcal/mol. Further, the docking scores (binding energy) of 1–20 compounds were compared with FDA-approved allosteric caspase inhibitors DICA and FICA as reference drugs. In the case of 1NME (caspase-3) target, the majority of the compounds showed good docking scores (> -7.0 kcal/mol) such as perulactone (1) (-9.1 kcal/mol), perulactone B (2) (-8.1 kcal/mol), pinocembrin (3) (-7.8 kcal/mol), myricetin (4) (-7.8 kcal/mol), naringenin (5) (-7.8 kcal/mol), ellagic acid (6) (-7.6 kcal/mol), galangin (7) (-7.9 kcal/mol), pinobanksin (8) (-7.5 kcal/mol), quercetin (9) (-7.8 kcal/mol), catechin (10) (-7.7 kcal/mol), kaempferol (11) (-7.8 kcal/mol), epicatechin (12) (-7.2 kcal/mol), procyanidin C1 (13) (-7.2 kcal/mol), and petunidin (14) (-7.3 kcal/mol) whereas reference molecules DICA and FICA exhibited relatively low docking scores as -5.0 and -5.1 kcal/mol, respectively. Herein, perulactone, having the highest docking score, was selected for a detailed study. Perulactone interacted with 1NME allosteric sites via three H-bonds (Asn208, Ser251, Asp253), one C-H bond (Glu248), four pi-alkyl bonds (Trp206, Trp214, Phe247, Phe256), and three

Table 1 ADMET properties of the 20 compounds using QikProp tool

Compounds (number)	MW	HBD	HBA	Log $P_{o/w}$	Log S	Log BB	Log HSA	HOA	Ro5
Perulactone (1)	518.6	3	9	3.76	-5.78	-1.73	0.68	3	1
Perulactone B (2)	488.6	4	8	2.88	-4.33	-1.45	0.30	3	Yes
Pinocembrin (3)	270.3	3	6	0.72	-2.27	-0.61	-0.38	3	Yes
Myricetin (4)	332.3	5	12	-2.2	-1.43	-2	-0.77	2	1
Naringenin (5)	286.3	4	8	-0.18	-1.96	-1.05	-0.55	3	Yes
Ellagic acid (6)	318.3	6	13	-2.39	-1.67	-1.56	-0.44	2	1
Galangin (7)	286.3	4	8	-0.04	-2.08	-0.95	-0.56	3	Yes
Pinobanksin (8)	286.3	4	8	0	-2.01	-0.88	-0.55	3	Yes
Quercetin (9)	318.3	6	11	-1.68	-1.60	-1.62	-0.68	2	1
Catechin (10)	302.3	5	10	-0.98	-1.77	-1.43	-0.65	2	Yes
Kaempferol (11)	302.3	5	10	-0.93	-1.70	-1.29	-0.66	2	Yes
Epicatechin (12)	302.3	5	10	-0.94	-1.75	-1.4	-0.62	2	Yes
Procyanidin C1 (13)	302.3	5	10	-0.93	-2.02	-1.61	-0.67	2	Yes
Petunidin (14)	332.3	5	11	-1.17	-1.65	-1.45	-0.73	2	Yes
Resveratrol (15)	242.3	3	5	0.98	-2.08	-1.04	-0.38	3	Yes
Ferulic acid (16)	204.2	3	6	-0.23	-0.76	-0.96	-0.81	2	Yes
<i>o</i> -Coumaric acid (17)	174.2	3	5	-0.08	-0.64	-0.82	-0.76	2	Yes
Gallic acid (18)	178.1	5	8	-1.92	-0.78	-1.42	-0.72	2	Yes
Protocatechuic acid (19)	162.1	4	6	-1.3	-0.54	-1.09	-0.81	2	Yes
Caffeic acid (20)	190.2	4	6	-0.91	-0.54	-1.27	-0.84	2	Yes

Yes, reveals no violation of Lipinski's rule whereas 1 states for one violation of Lipinski's rule

Table 2 The toxicity parameters of the 20 compounds

Compounds (number)	Mutagenic	Tumorigenic	Irritant	Reproductive effect
Perulactone (1)	No	No	No	Moderate
Perulactone B (2)	No	No	No	Moderate
Pinoembrin (3)	No	No	No	No
Myricetin (4)	Yes	No	No	No
Naringenin (5)	No	No	No	No
Ellagic acid (6)	No	No	No	No
Galangin (7)	Yes	No	No	No
Pinobanksin (8)	No	No	No	No
Quercetin (9)	Moderate	Moderate	No	No
Catechin (10)	No	No	No	No
Kaempferol (11)	No	No	No	No
Epicatechin (12)	No	No	No	No
Procyanidin C1 (13)	No	No	No	Yes
Petunidin (14)	No	No	No	No
Resveratrol (15)	No	No	No	No
Ferulic acid (16)	No	No	No	Moderate
<i>o</i> -Coumaric acid (17)	No	No	No	No
Gallic acid (18)	No	No	No	Yes
Protocatechuic acid (19)	No	No	No	No
Caffeic acid (20)	No	Moderate	No	Moderate

hydrophobic interactions (Ser209, Glu246, Phe252). On the other hand, DICA showed two H-bonds (Trp214), one pi-pi (Phe247), two pi-alkyl (Phe247), one pi-sulphur (Trp206), and eight hydrophobic (Arg207, Asn208, Ser209, Asp211, Gln217, Glu248, Ser249, and Phe250) interactions, whereas FICA exhibited one H-bond (Glu248), a C-H bond (Glu246), pi-pi (Trp206), halogen-bond (Arg207), van der Waal bond (Trp214), and five hydrophobic (Asn208, Ser209, Phe247, Ser247, Ser249, and Phe250) interactions. Comparing the docking scores and molecular interactions, amongst all compounds, perulactone is the most promising agent that binds effectively at allosteric sites of 1NME than that of DICA and FICA drugs. Figure 1A and Table 3 show detailed information on the docking scores of all the screened compounds and molecular interactions (2D and 3D) of the perulactone-1NME complex.

In the case of 3IBF (caspase-7) target, the majority of the compounds showed good docking scores (>-7.1 kcal/mol) such as perulactone (1) (-12.1 kcal/mol), perulactone B (2) (-9.7 kcal/mol), pinoembrin (3) (-8.0 kcal/mol), myricetin (4) (-8.0 kcal/mol), naringenin (5) (-8.0 kcal/mol), ellagic acid (6) (-8.0 kcal/mol), galangin (7) (-7.9 kcal/mol), pinobanksin (8) (-7.9 kcal/mol), quercetin (9) (-7.9 kcal/mol), catechin (10) (-7.9 kcal/mol), kaempferol (11) (-7.8 kcal/mol), epicatechin (12) (-7.8 kcal/mol), procyanidin C1 (13) (-7.7 kcal/mol), and petunidin (14) (-7.5 kcal/mol) whereas reference molecules DICA and FICA exhibited relatively low docking scores as -5.6 and -6.1 kcal/mol, respectively. Similarly, perulactone, having the highest docking score,

was selected for a detailed study. It was found that against 3IBF, perulactone showed three alkyl (Ile159, Lys160, Pro227), two pi-alkyl (Phe221, Phe521), and thirteen hydrophobic (Asn148, Thr163, Arg187, Tyr223, Val226, Tyr229, Val292, Asn448, Ile459, Lys460, Thr463, Glu516, Tyr523) molecular interactions. On the other side, DICA showed two H-bonds (Arg487, Tyr523), three alkyl bonds (Val226, Lys460, Met594), one pi-alkyl bond (Pro227), one pi-pi bond (Phe521), and four hydrophobic (Arg187, Val292, Thr463, Val592) interactions, while FICA binds via two H-bonds (Arg487, Tyr523), two pi-alkyl bonds (Pro227, Val592), one pi-pi bond (Phe521), one halogen bond (Glu516), and four hydrophobic (Arg187, Val292, Pro527, Met594) interactions at the allosteric sites (Ansari et al. 2022a, b). Comparing the docking scores and molecular interactions, amongst all compounds, perulactone is the most promising agent that binds effectively at allosteric sites of 3IBF than that of DICA and FICA drugs. Figure 1B and Table 3 show detailed information on the docking scores of all the screened compounds and molecular interactions (2D and 3D) of the perulactone-3IBF complex.

Overall, perulactone had the highest docking score and a higher number of molecular interactions when compared to DICA and FICA, facilitating its functionalities to be tightly bound at allosteric sites of both the 1NME and 3IBF receptors. Furthermore, to explore the binding strengths of Perulactone within the binding pockets of 1NME and 3IBF, a molecular dynamic simulation study was performed for Perulactone-1NME and Perulactone-3IBF complexes.

Table 3 Binding affinity list of selected 20 berries compounds and control drugs

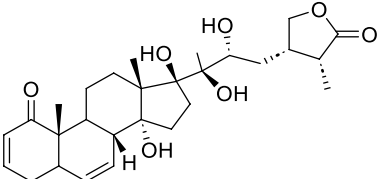
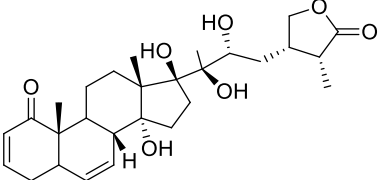
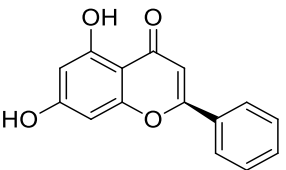
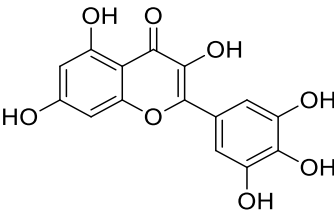
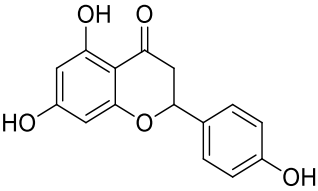
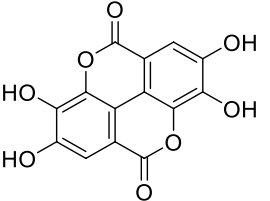
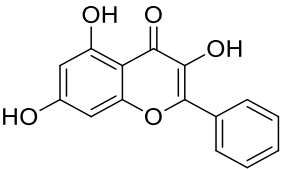
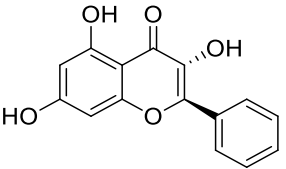
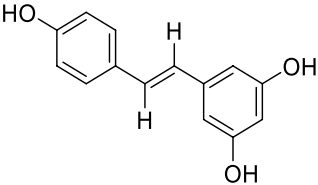
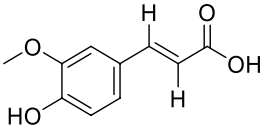
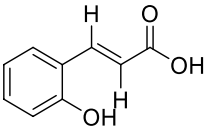
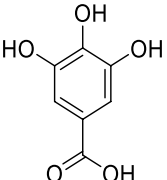
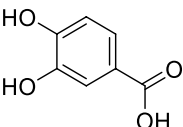
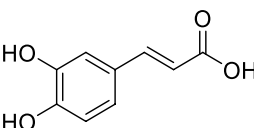
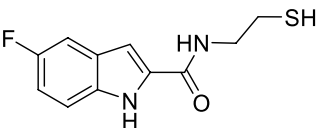
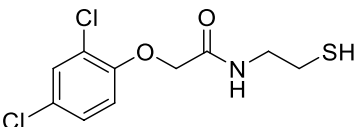
Compound number	Structure	Source	BA (1NME) (kcal/mol)	BA (3IBF) (kcal/mol)
1		Cape gooseberry	-9.1	-12.1
2		Cape gooseberry	-8.1	-9.7
3		Blackberry	-7.8	-8.0
4		Blueberries	-7.8	-8.0
5		Golden berry	-7.8	-8.0
6		Golden berry	-7.6	-8.0
7		Blackberry	-7.9	-7.9
8		Blackberry	-7.5	-7.9

Table 3 (continued)

Compound number	Structure	Source	BA (1NME) (kcal/mol)	BA (3IBF) (kcal/mol)
9		Blueberries	-7.8	-7.9
10		Golden berry	-7.7	-7.9
11		Blueberries	-7.8	-7.8
12		Golden berry	-7.2	-7.8
13		Elderberry	-7.2	-7.7
14		Blueberries	-7.3	-7.5

Table 3 (continued)

Compound number	Structure	Source	BA (1NME) (kcal/mol)	BA (3IBF) (kcal/mol)
15		Golden berries	-6.2	-7.1
16		Golden berries	-5.3	-6.0
17		Golden berries	-5.2	-6.0
18		Golden berries	-5.6	-5.5
19		Golden berries	-5.4	-5.5
20		Honeysuckle berries	-5.1	-5.5
FICA		Control drug	-5.1	-6.1
DICA		Control drug	-5.0	-5.6

BA binding energy, 1NME PDB ID of caspase-3, 3IBF PDB ID of caspase-7

Molecular dynamic simulation

The MD simulation analyzes the ligand–protein interactions' stability and conformational changes. In this study, we measured the RMSD (root mean square deviation), RMSF (root mean square fluctuation), SSE (secondary structure elements), Rg (radius of gyration), MolSA (molecular surface area), SASA (solvent accessible surface area), and PSA (polar surface area) of Perulactone-1NME and Perulactone-3IBF complexes for 100 ns MD simulation in triplicate.

RMSD and RMSF analysis

The RMSD values of the Perulactone-3IBF complex were observed between 1.270–3.088 Å and 1.011–2.069 Å for ligand and protein, as depicted in Table 4. The perulactone showed very compact binding within the active site due to less deviation (Fig. 2A), and it achieved equilibrium from the initial to the end of the simulation. The ligand indicated strong interactions, including H-bonds to Arg487 (62%), Glu216 (74%), water-bridges to Arg187 (74%), Glu447

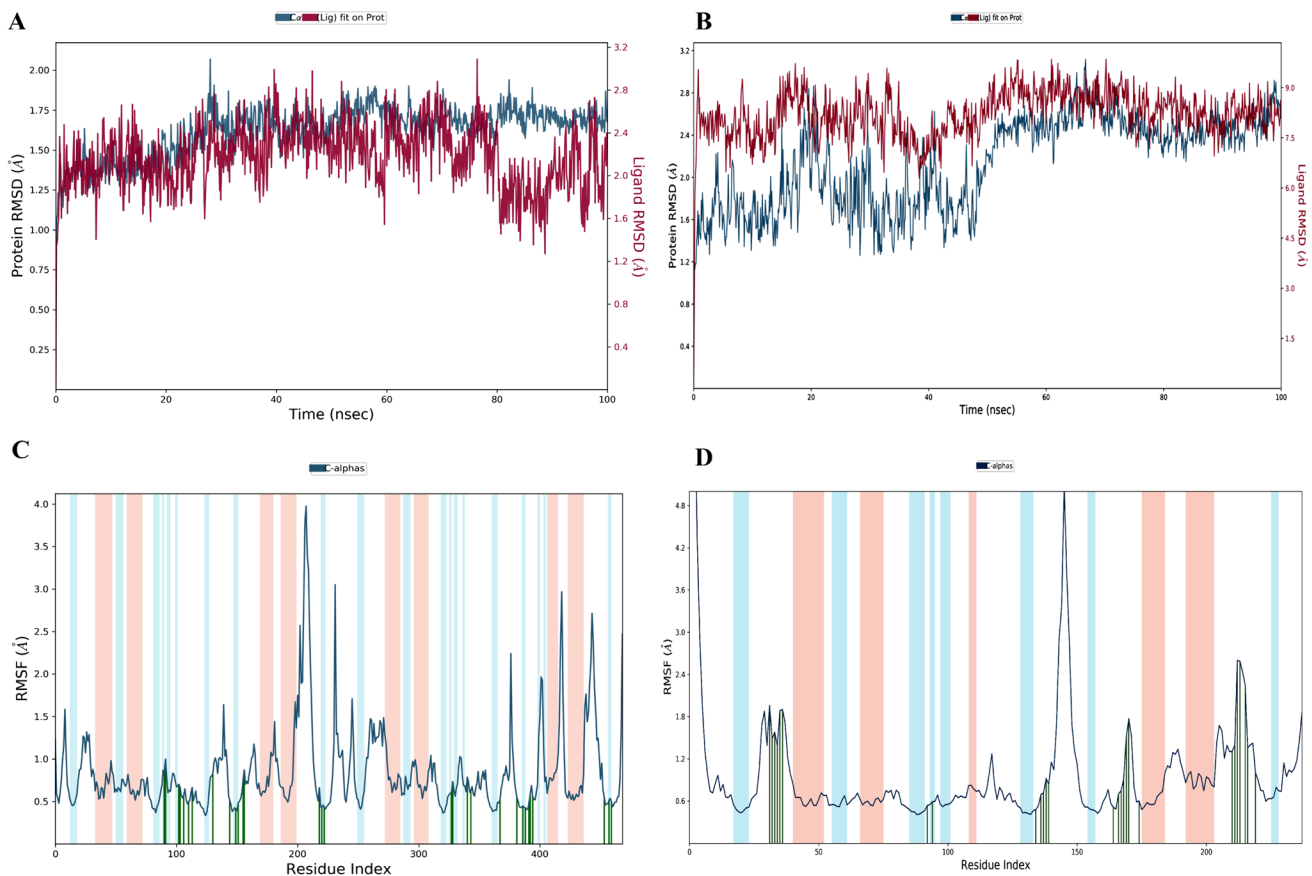
Table 4 MD simulation parameters of perulactone compound with 3IBF, and 1NME proteins

Analysis	Perulactone-3IBF	Perulactone-1NME
C α RMSD(Å)	1.011–2.069	1.129–3.156
Ligand RMSD (Å)	1.270–3.088	2.426–9.850
C α RMSF (Å)	0.334–3.977	0.408–10.378
rGyr (Å)	5.110–5.726	4.875–5.720
MolSA (Å ²)	444.100–465.672	440.270–462.313
SASA(Å ²)	66.244–260.166	208.309–492.363
PSA (Å ²)	177.744–218.159	180.012–206.505

(75%), Pro527 (37%), and Phe221, which showed hydrophobic interaction to the end of the simulation (Fig. 3A). Secondly, we analyzed the perulactone-1NME complex, showing the RMSD values range from 2.426–9.850 Å and 1.129–3.156 Å for ligand and protein respectively (Table 4). During the simulation, the perulactone deviated from the initial position to 9.540 Å because it bound with the amino acids in the loop region for a small time period (0.80 ns). In Figs. 2B and 3B, perulactone showed the stability through

binding within the β -strand region via displaying the H-bond to Ser209 (57%), three water-bridges to Trp206 (36%), Arg207 (33%), Phe250 (30%), and hydrophobic interaction to Tyr204, and Phe256 amino acids of the receptor. Thus, the values of RMSD stated that perulactone forms stable bindings within the 3IBF and 1NME protein receptors (Ansari et al. 2023; Alhakamy et al. 2023).

The RMSF explores the resiliency of the amino acids in proteins. The higher fluctuations of amino acids reveal more flexibility, whereas the lesser fluctuations of amino acids indicate the more compactness of ligands in the active sites of proteins. To check the compactness of perulactone within the 3IBF and 1NME proteins, the RMSF values were found as 0.334–3.997 Å, and 0.408–10.378 Å for perulactone-3IBF, and perulactone-1NME complexes respectively. As depicted in Table 4 as well as Fig. 2C and D, Moreover, high fluctuations were noticed in the loop regions of the active site of caspase 7 including Gln603, Gln303, Glu365, and Asp578 amino acids whereas the fluctuation took place between Thr174, Lys186 amino acids of caspase 3 during the whole duration of simulation as displayed (Sheikh et al. 2023a, b; Sepehri et al. 2022).

**Fig. 2** The RMSD plots **A** perulactone-3IBF ligand–protein complex, **B** perulactone-1NME ligand–protein complex, and RMSF plots **C** perulactone-3IBF ligand–protein complex, **D** perulactone-1NME ligand–protein complex

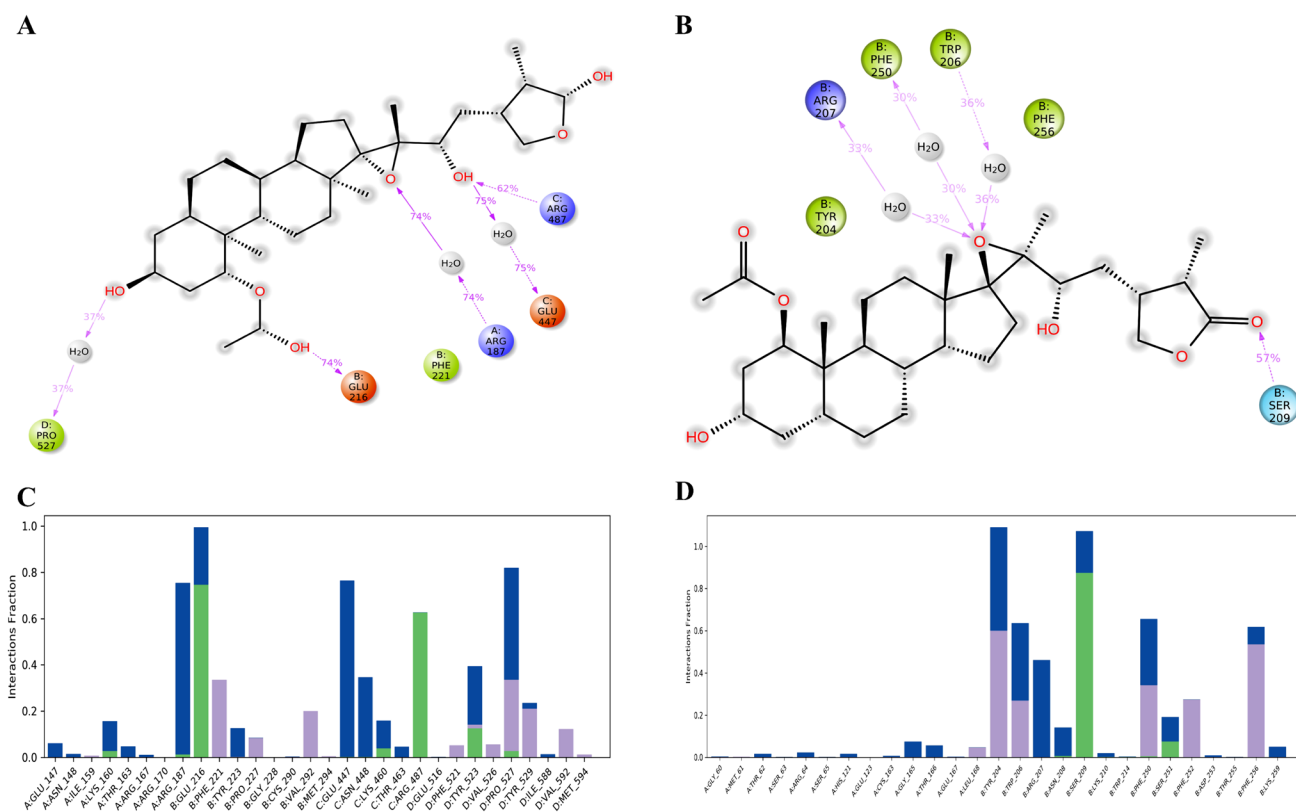


Fig. 3 Ligand interactions: **A** perulactone-3IBF ligand–protein complex, **B** perulactone-1NME ligand–protein complex and Bar charts of ligand interactions of **C** perulactone-3IBF ligand–protein complex, **D** perulactone-1NME ligand–protein complex

Analysis of secondary structure elements (SSE)

The secondary structure elements (SSE) were explored for the variations in the α -helices and β -strand amino acids that arise during MD simulation. The α -helices and β -strand amino acids were monitored for both the complexes such as perulactone-3IBF, and perulactone-1NME. To this, it had been observed that the total percentage of SSE involved 39.53% comprising 21.91% α -helices and 17.62% β -strand, among the total percentage of SSE for the perulactone-3IBF complex, while 37.80% percent, which included 20.58% α -helices and 17.23% β -strand of total SSE was found for perulactone-1NME (Table 5). Thus, perulactone-3IBF complex showed lesser changes in amino acids of the active sites of 3IBF due to α -helices and β -strands (Fig. 4A), whereas more fluctuations were observed in the perulactone-1NME complex due to large loop regions of amino acids over the simulation (Fig. 4B) (Abdalla et al. 2022).

Radius of gyration (Rg) analysis

The radius of gyration (Rg) is a crucial parameter that defines the folding of ligands in the ligand–protein complex in MD simulation evaluation. In the current study, the

Table 5 Percentage of secondary structure regions amino acid distribution of 3IBF and 1NME proteins throughout 100 ns MD simulations

Complexes	% Alpha-helices	% Beta-strands	% Total SSE
Perulactone-3IBF	21.91	17.62	39.53
Perulactone-1NME	20.58	17.23	37.80

calculated values of Rg were found to range from 5.110 to 5.726 Å, and 4.875 to 5.720 Å for perulactone-3IBF, and perulactone-1NME complexes, respectively (Table 4). It indicates that perulactone exhibits robust compactness against both the proteins 3IBF and 1NME over the 100 ns simulation (Ansari et al. 2022a, b).

Solvent accessible surface area (SASA), molecular surface area (MolSA), and polar surface area (PSA) analyses

SASA, MolSA, and PSA discuss the accessible water molecules (equivalent to vander Waal area), molecular surface area and solvent-accessible surface area contributed by the polar (oxygen, nitrogen) atoms of the ligand during the

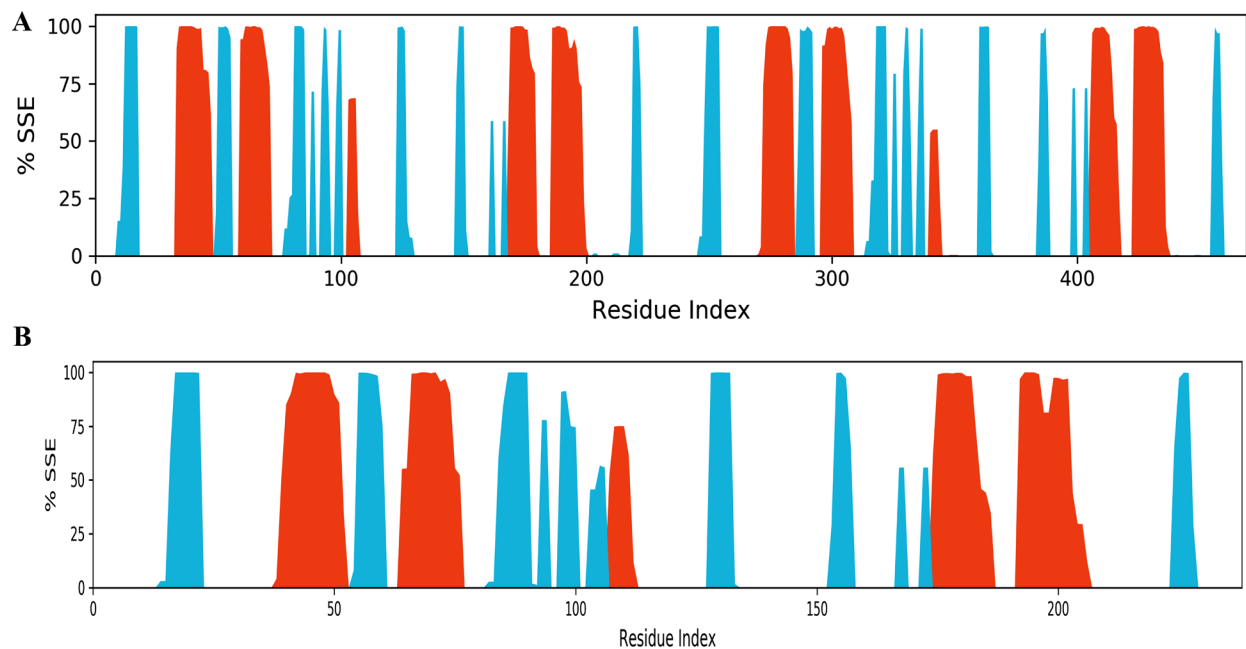


Fig. 4 The plots of secondary structure elements (SSE) such as α -helices (orange colour) and β -strands (colour) involved for the ligand–protein complexes: **A** perulactone-3IBF ligand–protein complex, **B** perulactone-1NME ligand–protein complex during the 100 ns MD simulation

simulation trajectory, respectively. As depicted in Fig. 5 and Table 4, the SASA values (66.244–260.166 \AA^2 , and 208.309–492.363 \AA^2), MolSA values (444.100–465.672 \AA^2 , and 440.270–462.313 \AA^2) well as the PSA values (177.744–218.159 \AA^2 , and 180.012–206.505 \AA^2), appeared for perulactone-3IBF and Perulactone-1NME respectively, throughout the simulation (Umar et al. 2022).

MMGBSA analysis

To calculate the free binding energy of the ligand–protein complex, we implemented the MMGBSA approach, which enumerates the free binding energy of the ligand with the targeted receptor. The lowest binding energy interprets the most reliable and stable ligand in the active site of the

receptor (Tuccinardi 2021). Now, we estimated the pre- and post-simulation free binding energy of lead compounds against the targeted receptors (Table 6). Consequently, we obtained the values of the lowest Gibbs (ΔG) free energy -62.35 kcal/mol and -66.32 kcal/mol for perulactone-3IBF and perulactone-1NME complexes, respectively. Similarly, the control drugs DICA and FICA revealed Gibbs's (ΔG) free energy (-45.29 , and -39.51 kcal/mol) and (-26.37 , and -15.50 kcal/mol). As a result, the perulactone manifested a more stable candidate than the control drugs Dica and Fica against the targeted receptors (Kausar and Nayeem 2018). All of the screened compounds (1–20) fit Lipinski's rule and other ADMET properties that are required to fulfill the necessary conditions as potent drug leads. We proposed these drugs as effective allosteric caspase-3/-7 inhibitors for

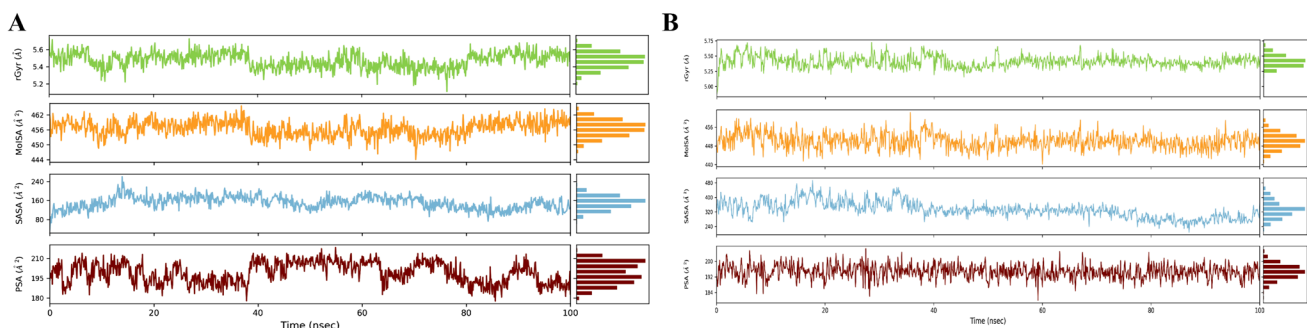


Fig. 5 Ligand properties of **A** perulactone with 3IBF protein ligand–protein complex, and **B** perulactone with 1NME ligand–protein complex for 100 ns simulation

Table 6 Estimation of MMGBSA energies of the perulactone compound against 3IBF, and 1NME proteins

Compounds	Parameters (PDB ID:3IBF)				Parameters (PDB ID:1NME)			
	ΔG_{Bind}	ΔG_{Coul}	ΔG_{GB}	ΔG_{vdW}	ΔG_{Bind}	ΔG_{Coul}	ΔG_{GB}	ΔG_{vdW}
Perulactone	-63.98	-17.41	57.08	-48.31	-66.32	-16.47	29.32	-35.76
Dica	-45.16	-12.12	20.36	-30.58	-39.51	-18.09	18.06	-24.63
Fica	-26.37	-25.83	27.44	-16.05	-15.50	-21.26	25.82	-16.28

controlling the apoptosis process. As a result, our findings could help forward research into berry fruit components as anti-apoptotic medications for treating a variety of diseases. Furthermore, we are the first to report on perulactone and other phenolic compounds that serve as better allosteric inhibitors than FICA and DICA drug molecules.

Researchers have found that caspase-3 and -7 allosteric inhibition, which offer the majority of cleavage during apoptosis and govern cell proliferation and differentiation during the cell cycle, is crucial in the treatment of a range of diseases (Murakami et al. 2013). Undoubtedly, the mechanism of apoptosis and inflammation can be better understood with the use of caspase inhibitors. However, synthetic FDA-approved caspase inhibitors have failed clinical studies due to considerable adverse effects, lack of efficacy, poor target specificity and/or selectivity, as the majority of them bind to orthosteric sites (Kudelova et al. 2015). To get over these limitations, targeting allosteric regions in the development of therapeutic drugs for apoptosis-related diseases may be a promising option. As discussed in the “Introduction” section, plant-derived compounds, on the other hand, may be a safer and more effective therapeutic agent for dealing with these issues because they are less expensive and have few, if any, adverse effects. Although several studies have indicated the potential function of compounds derived from plants in inhibiting caspase-3 and caspase-7 at orthogonic regions, allosteric site inhibition and the molecular mechanism of those medications are still to be studied (Garner et al. 2019).

Computer-based research is an established strategy for identifying and developing therapeutic agents for a variety of diseases. In the current study, we used virtual screening to find allosteric caspase-3 and caspase-7 inhibitors among 100 compounds derived from berry fruits, including polyphenols, flavonoids, and withanolides. Prior to molecular docking and molecular dynamic simulation investigations, a library of 100 compounds of berry fruits was evaluated using ADMET. In addition to toxicity measures, Lipinski's rule of five (Ro5) was used to evaluate the drug-like properties. Twenty compounds (1–20) were taken out of this for additional molecular docking and molecular dynamic simulation analyses. Four of these compounds—perulactone (1), myricetin (4), ellagic acid (6), and quercetin (9) were shown to defy Ro5 by a single parameter, as Table 1 illustrates. However, according to Ro5, compounds with no or at least one violation can be successfully implemented

as therapeutically relevant medicines. Thus, the current ADMET study revealed that 1–20 compounds had therapeutic characteristics and good oral bioavailability. Following that, to analyse the molecular interactions of compounds (1–20), molecular docking experiments were performed at caspase-3 and caspase-7 allosteric sites to explore binding mechanisms. Our docking investigation revealed that the complexes contained many different kinds of molecular interactions, including H-bonds, hydrophobic contacts, π - π contacts, cation- π contacts, and salt-bridges. As shown in Table 2, compounds 1–20 demonstrated strong binding efficacy (high negative binding energies) within the allosteric pockets of each of the monomers of caspase-3 and caspase-7 receptors as compared to DICA and FICA as reference compounds. The withanolides, namely perulactone and perulactone B, obtained from cape gooseberry fruits exhibited the highest binding energies of -9.1 and -8.1 kcal/mol against caspase-3 (1NME), whereas -12.7 and -9.7 kcal/mol against caspase-7 (3IBF), respectively. The docking results of perulactone were comparable to previous experimental and virtual data, where they were associated with Arg187 residue of caspase-3 and Arg207 residue of caspase-7 via cation- π contact, as in FDA-approved DICA and FICA drugs. Since the chemical structure of perulactone contains four hydroxyl groups, one lactone ring, and one COCH3 functionality, the formation of hydrogen bonds and salt bridges with essential amino acid residues may further facilitate the allosteric binding of perulactone. Our analysis revealed that the hydroxyl moiety of the lactone ring hinged with the Asn208 residue while the COCH3 functional group interacted with the Ser251 and Asp253 residues through hydrogen bonding in the S4 pocket of caspase-3. It resembled a naturally occurring caspase-3 inhibitor ligand. Additionally, the smaller S2 pocket, which has residues of Trp206 and Phe250 that function as active sites in the S4 pocket was produced by the S4 pocket. (Minini et al. 2017). On the other hand, during the molecular interactions of perulactone and caspase-7, we discovered that the molecular interactions of perulactone were similar to the native tetrapeptide inhibitors in the allosteric regions. Because Tyr223 and Arg187 are necessary for cleaving the active site, the perulactone exhibited aliphatic engagement, a hydrophobic interaction that migrated away from the site. (Hardy et al. 2004). The molecular interactions identified in our molecular docking study were compared to compounds found in

the literature. In an *in vitro* investigation, we observed that quinolone-based drugs, such as quinoline-2-one/pyrazole, suppress caspase-3 via interactions of quinoline C=O and pyrazole C=N functionality with the Arg207 and Gly122 residues, whereas *N*-acetyl cysteine interacted with Arg207, Gly122 and Arg64 residues through hydrogen bonding (Aly et al. 2020). Similarly, in a further investigation, the anti-apoptotic activity of 6-methoxy-4-(4-((2-oxo-1,2-dihydroquinolin-4-yl)oxy)methyl) was uncovered by Essmat M. El-Sheref et al. after they designed and synthesized some 1,2,3-triazole/Bis-2(1*H*)-quinolinone derivatives such as 1,2,3-triazol-1-yl-quinolin-2(1*H*)-one against caspase-3 inhibition in the rat testis serum. Using molecular docking analysis, this study demonstrated that the quinoline NH and triazole C=N functionalities of the chemical interacted with the amino acids Thr140, Gly125, and Lys137 in the catalytic site of caspase-3, resulting in higher stability than the reference molecule *N*-acetylcysteine. When we compared our findings to the literature, we observed that perulactone was better at showing the molecular interaction with Arg187 and Arg207 residues in the allosteric sites of caspase-3 and -7, respectively.

Furthermore, a molecular dynamic (MD) simulation study of perulactone within the binding pockets of 1NME and 3IBF receptors was performed over a 100 ns period. In MD simulation, we evaluated the RMSD, RMSF, SSE, Rg, MolSA, SASA, and PSA parameters to gain insight into the stability of perulactone-1NME and perulactone-3IBF complexes. For the perulactone-3IBF complex, Table 4 and Fig. 5 displayed the RMSD value between 1.270–3.088 Å and 1.011–2.069 Å, while for the perulactone-1NME complex, the values were between 2.426–9.850 Å and 1.129–3.156 Å. According to these results, both complexes were compact within the binding pockets. It has been found recently that RMSD values between 2.0 and 3.0 Å may maintain the complexes in the appropriate orientation, but RMSD values less than 2.0 Å are well connected with favourable docking scores (Ramírez and Caballero 2018). The RMSF is used to observe the fluctuation of ligands within protein pockets. Our investigation found that perulactone-3IBF and perulactone-1NME complexes had RMSF values of 0.334–3.997 Å and 0.408–10.378 Å, respectively. According to the prior study, no fluctuations should be noticed within 3.0 Å. In the current investigation, the perulactone-3IBF complex was stable because it was compact within a range of 3.0 Å (De Vita et al. 2021). Furthermore, the values of additional parameters such as SSE, Rg, MolSA, SASA, and PSA were found to be significant for both perulactone-3IBF and perulactone-1NME complexes, and they were in good agreement with those reported in the prior literature (Ferdousi et al. 2022). Finally, we used the MMGBSA method to redock the perulactone-3IBF and perulactone-1NME complexes to validate our docking results. Using this approach,

we found that the perulactone-3IBF and perulactone-1NME complexes have the lowest Gibbs (G) free energy compared to DICA and FICA. We conclude, based on the analysis of the docking scores and stability parameters, that perulactone, the main compound of cape gooseberry fruit, is a more promising candidate than the other compounds (2–20) that were investigated as an allosteric inhibitor of caspase-3 and caspase-7. However, additional research using *in vitro* and *in vivo* studies is required to further exploration of perulactone and related compounds to identify allosteric caspase-3 and caspase-7 inhibitors for the treatment of apoptosis-related diseases in the coming years.

Conclusion

To identify possible plant-derived compounds as allosteric inhibitors of caspase-3/-7, a library of 100 compounds from berry fruits was prepared based on the pharmacological activities regarding caspase inhibitions. The compounds were then assessed by computer investigations using ADMET, molecular docking, MD simulation, and MMGBSA calculations. Twenty compounds (1–20) and other FDA-approved compounds that were listed in the literature performed better in docking scores after ADMET screening than the reference drug molecules, DICA and FICA. Perulactone demonstrated significant docking scores of –9.1 and –12.1 kcal/mol against caspase-3 and -7, respectively, in the molecular docking study. In contrast, DICA and FICA demonstrated weak docking scores of –5.0 and –5.1 kcal/mol against caspase 3 and –5.6 and –6.1 kcal/mol against caspase 7, respectively. Furthermore, perulactone produced strong binding complexes and showed notable stability inside the allosteric domains of the 3IBF and 1NME targets with the help of the MD simulation approach. These findings were confirmed by redocking MMGBSA calculations. Briefly, our research suggests that perulactone might be a more potent allosteric inhibitor of the caspase-3/-7 proteins that are involved in the process of apoptosis. Numerous links between perulactone and the reference drug molecules in the caspase-3/-7 allosteric regions, along with other interactions, supported our study. It is suggested that perulactone and other compounds from berry fruits may be recommended for further *in-vitro* and *in-vivo* studies.

Supplementary Information The online version contains supplementary material available at <https://doi.org/10.1007/s13205-024-04067-7>.

Acknowledgements The authors would like to express their gratitude to the management teams of Era University in Lucknow (India) and the American University of Barbados (AUB) for their cooperation with this research endeavor.

Author contributions M.F.K. and M.A.K. designed, conceptualized, and supervised the study; W.A.A. and S.M.M.H. carried out the

computational study, data interpretation, and wrote the manuscript; Z.S. S.A and M.S.K. reviewed the manuscript and analyzed the data of this work. All authors have read the final draft of the manuscript and agreed to the published version of the manuscript.

Funding The generous support from the research-supporting project (RSP2024R352) by the King Saud University, Riyadh, Kingdom of Saudi Arabia, and the authors are very thankful to Era's Lucknow Medical College & Hospital, Era University, Lucknow (India) for assisting with intramural funding (R-Cell/2024/184) to carry out this work.

Data availability The computational data associated with this research work has been produced in our institute with the assistance of the necessary systems and reported accordingly in the manuscript.

Declarations

Conflict of interest The authors declare no conflict of interest.

References

- Abdalla M, Eltayb WA, El-Arabey AA, Singh K, Jiang X (2022) Molecular dynamic study of SARS-COV-2 with various S protein mutations and their effect on thermodynamic properties. *Comput Biol Med* 141:105025. <https://doi.org/10.1016/j.combiomed.2021.105025>
- Abdullah A, Ravanan P (2018) Kaempferol mitigates endoplasmic reticulum stress induced cell death by targeting caspase 3/7. *Sci Rep* 8(1):2189. <https://doi.org/10.1038/s41598-018-20499-7>
- Agniswamy J, Fang B, Weber IT (2009) Conformational similarity in the activation of caspase-3 and -7 revealed by the unliganded and inhibited structures of caspase-7. *Apoptosis* 14(10):1135–1144. <https://doi.org/10.1007/s10495-009-0388-9>
- AlAli M, Alqubaisy M, Aljaafari MN, AlAli AO, Baqais L, Molouki A, Abushelaibi A, Lai K-S, Lim S-HE (2021) Nutraceuticals: transformation of conventional foods into health promoters/disease preventers and safety considerations. *Molecules* 26(9):2540. <https://doi.org/10.3390/molecules26092540>
- Alghamdi A, Abouzzied AS, Alamri A, Anwar S, Ansari M, Khadra I, Zaki YH, Gomha SM (2023) Synthesis, molecular docking, and dynamic simulation targeting main protease (M^{pro}) of new, thiazole clubbed pyridine scaffolds as potential COVID-19 inhibitors. *Curr Issues Mol Biol* 45(2):1422–1442. <https://doi.org/10.3390/cimb45020093>
- Alhakamy NA, Saquib M, Sanobar KMF, Ansari WA, Arif DO, Irfan M, Khan MI, Hussain MK (2023) Natural product-inspired synthesis of coumarin–chalcone hybrids as potential anti-breast cancer agents. *Front Pharmacol* 14:1231450. <https://doi.org/10.3389/fphar.2023.1231450>
- Aly AA, Sayed SM, Abdelhafez EMN, Abdelhafez SMN, Abdelzaher WY, Raslan MA, Ahmed AE, Thabet K, El-Reedy AAM, Brown AB, Bräse S (2020) New quinoline-2-one/pyrazole derivatives; design, synthesis, molecular docking, anti-apoptotic evaluation, and caspase-3 inhibition assay. *Bioorg Chem* 94:103348. <https://doi.org/10.1016/j.bioorg.2019.103348>
- Ansari WA, Ahmad T, Khan MA, Khan ZA, Khan MF (2022a) Exploration of luteolin as potential anti-covid-19 agent: molecular docking, molecular dynamic simulation, ADMET and DFT analysis. *Lett Drug Des Discov* 19(8):741–756. <https://doi.org/10.2174/1570180819666211222151725>
- Ansari WA, Khan MA, Rizvi F, Ali K, Hussain MK, Saquib M, Khan MF (2022b) Computational screening of plant-derived natural products against SARS-COV-2 variants. *Fut Pharmacol* 2(4):558–578. <https://doi.org/10.3390/futurepharmacol2040034>
- Ansari WA, Rab SO, Saquib M, Sarfraz A, Hussain MK, Akhtar MS, Ahmad I, Khan MF (2023) Pentafuhalol-B, a phlorotannin from brown algae, strongly inhibits the PLK-1 overexpression in cancer cells as revealed by computational analysis. *Molecules* 28(15):5853. <https://doi.org/10.3390/molecules28155853>
- Baby B, Antony P, Vijayan R (2017) Antioxidant and anticancer properties of berries. *Crit Rev Food Sci Nutr* 58(15):2491–2507. <https://doi.org/10.1080/10408398.2017.1329198>
- Bader Ul Ain H, Tufail T, Javed M, Tufail T, Arshad MU, Hussain M, Gull Khan S, Bashir S, Al Jbawi E, Abdulaali Saewan S (2022) Phytochemical profile and pro-healthy properties of berries. *Int J Food Prop* 25(1):1714–1735. <https://doi.org/10.1080/10942912.2022.2096062>
- Becker JW, Rotonda J, Soisson SM, Aspiotis R, Bayly C, Francoeur S, Gallant M, Garcia-Calvo M, Giroux A, Grimm E, Han Y, McKay D, Nicholson DW, Peterson E, Renaud J, Roy S, Thornberry N, Zamboni R (2004) Reducing the peptidyl features of caspase-3 inhibitors: a structural analysis. *J Med Chem* 47(10):2466–2474. <https://doi.org/10.1021/jm0305523>
- Brentnall M, Rodriguez-Menocal L, De Guevara RL, Cepero E, Boise LH (2013) Caspase-9, caspase-3 and caspase-7 have distinct roles during intrinsic apoptosis. *BMC Cell Biol* 14:32. <https://doi.org/10.1186/1471-2121-14-32>
- Chaudhry G-S, Akim AM, Sung YY, Muhammad TS (2022) Cancer and apoptosis. *Methods Mol Biol* 2543:191–210. https://doi.org/10.1007/978-1-0716-2553-8_16
- Chien SY, Wu YC, Chung JG, Yang JS, Lu HF, Tsou MF, Wood WG, Kuo SJ, Chen DR (2009) Quercetin-induced apoptosis acts through mitochondrial- and caspase-3-dependent pathways in human breast cancer MDA-MB-231 cells. *Hum Exp Toxicol* 28(8):493–503. <https://doi.org/10.1177/0960327109107002>
- Cho H, Jung H, Lee H, Yi HC, Kwak H, Hwang KT (2015) Chemopreventive activity of ellagitannins and their derivatives from black raspberry seeds on HT-29 colon cancer cells. *Food Funct* 6(5):1675–1683. <https://doi.org/10.1039/c5fo00274e>
- Conn PJ, Christopoulos A, Lindsley CW (2009) Allosteric modulators of GPCRs: a novel approach for the treatment of CNS disorders. *Nat Rev Drug Discov* 8(1):41–54. <https://doi.org/10.1038/nrd2760>
- Danbara N, Yuri T, Tsujita-Kyutoku M, Sato M, Senzaki H, Takada H, Hada T, Miyazawa T, Okazaki K, Tsubura A (2004) Conjugated docosahexaenoic acid is a potent inducer of cell cycle arrest and apoptosis and inhibits growth of Colo 201 human colon cancer cells. *Nutr Cancer* 50(1):71–79. https://doi.org/10.1207/s15327914nc5001_10
- Dang Q, Song W, Xu D, Ma Y, Li F, Zeng J, Zhu G, Wang X, Chang LS, He D, Li L (2015) Kaempferol suppresses bladder cancer tumor growth by inhibiting cell proliferation and inducing apoptosis. *Mol Carcinog* 54(9):831–840. <https://doi.org/10.1002/mc.22154>
- De Vita S, Chini MG, Bifulco G, Lauro G (2021) Insights into the ligand binding to bromodomain-containing protein 9 (BRD9): a guide to the selection of potential binders by computational methods. *Molecules* 26(23):7192. <https://doi.org/10.3390/molecules26237192>
- Duthie SJ, Gardner PT, Morrice PC, Wood SG, Pirie L, Bestwick CC, Milne L, Duthie GG (2004) DNA stability and lipid peroxidation in vitamin E-deficient rats in vivo and colon cells in vitro. *Eur J Nutr* 44:195–203. <https://doi.org/10.1007/s00394-004-0511-1>
- Elisia I, Kitts DD (2008) Anthocyanins inhibit peroxyl radical-induced apoptosis in Caco-2 cells. *Mol Cell Biochem* 312:139–145. <https://doi.org/10.1007/s11010-008-9729-1>
- Erlanson DA, Lam JW, Wiesmann C, Luong TN, Simmons RL, DeLano WL, Choong IC, Burdett MT, Flanagan WM, Lee D, Gordon EM, O'Brien T (2003) In situ assembly of enzyme

- inhibitors using extended tethering. *Nat Biotechnol* 21(3):308–314. <https://doi.org/10.1038/nbt786>
- Ferdausi N, Islam S, Rimiti FH, Quayum ST, Arshad EM, Ibnat A, Islam T, Arefin A, Ema TI, Biswas P, Dey D, Azad SA (2022) Point-specific interactions of isovitexin with the neighboring amino acid residues of the hACE2 receptor as a targeted therapeutic agent in suppressing the SARS-CoV-2 influx mechanism. *J Adv Vet Anim Res* 9(2):230–240. <https://doi.org/10.5455/javar.2022.i588>
- Ferguson PJ, Kurowska E, Freeman DJ, Chambers AF, Koropatnick DJ (2004) A flavonoid fraction from cranberry extract inhibits proliferation of human tumor cell lines. *J Nutr* 134(6):1529–1535. <https://doi.org/10.1093/jn/134.6.1529>
- Garner TP, Amgalan D, Reyna DE, Li S, Kitsis RN, Gavathiotis E (2019) Small-molecule allosteric inhibitors of BAX. *Nat Chem Biol* 15(4):322–330. <https://doi.org/10.1038/s41589-018-0223-0>
- Golovinskaia O, Wang C-K (2021) Review of functional and pharmacological activities of berries. *Molecules* 26(13):3904. <https://doi.org/10.3390/molecules26133904>
- Green DR, Llambi F (2015) Cell death signaling. *Cold Spring Harb Perspect Biol* 7:1–24. <https://doi.org/10.1101/cshperspect.a006080>
- Häcker H-G, Sisay MT, Gütschow M (2011) Allosteric modulation of caspases. *Pharmacol Ther* 132(2):180–195. <https://doi.org/10.1016/j.pharmthera.2011.07.003>
- Hardy JA, Lam J, Nguyen JT, O'Brien T, Wells JA (2004) Discovery of an allosteric site in the caspases. *PNAS* 101(34):12461–12466. <https://doi.org/10.1073/pnas.0404781101>
- Henrich CJ, Brooks AD, Erickson KL, Thomas CL, Bokesch HR, Tewary P, Thompson CR, Pompei RJ, Gustafson KR, McMahon JB, Sayers TJ (2015) Withanolide E sensitizes renal carcinoma cells to TRAIL-induced apoptosis by increasing cFLIP degradation. *Cell Death Dis* 6(2):e1666. <https://doi.org/10.1038/cddis.2015.38>
- Jung YY, Um JY, Chinnathambi A, Govindasamy C, Narula AS, Namjoshi OA, Blough BE, Sethi G, Ahn KS (2022) Withanolide modulates the potential crosstalk between apoptosis and autophagy in different colorectal cancer cell lines. *Eur J Pharmacol* 928:175113. <https://doi.org/10.1016/j.ejphar.2022.175113>
- Kausar T, Nayeem SM (2018) Identification of small molecule inhibitors of ALK2: a virtual screening, density functional theory, and molecular dynamics simulations study. *J Mol Model* 24:262. <https://doi.org/10.1007/s00894-018-3789-2>
- Kesavardhana S, Malireddi RKS, Kanneganti T-D (2020) Caspases in cell death, inflammation, and pyroptosis. *Annu Rev Immunol* 38:567–595. <https://doi.org/10.1146/annurev-immunol-073119-095439>
- Khan MF, Khan MA, Khan ZA, Ahamad T, Ansari WA (2021) In-silico study to identify dietary molecules as potential SARS-COV-2 agents. *Lett Drug Des Discov* 18(6):562–573. <https://doi.org/10.2174/1570180817999201209204153>
- Khan MF, Ansari WA, Ahamad T, Khan MA, Khan ZA, Sarfraz A, Khan MA (2022a) Bioactive components of different nasal spray solutions may defeat SARS-COV2: repurposing and in Silico Studies. *J Mol Model* 28:212. <https://doi.org/10.1007/s00894-022-05213-9>
- Khan MF, Ansari WA, Rizvi F, Khan MA, Khan ZA (2022b) Computational study reveals the inhibitory effects of chemical constituents from *Azadirachta indica* (indian neem) against Delta and Omicron variants of SARS-COV-2. *Coronaviruses* 3(5):62–72. <https://doi.org/10.2174/2666796703666220827100054>
- Krishna Deepak RN, Abdullah A, Talwar P, Fan H, Ravanan P (2018) Identification of fda-approved drugs as novel allosteric inhibitors of human executioner caspases. *Proteins* 86(11):1202–1210. <https://doi.org/10.1002/prot.25601>
- Kudelova J, Fleischmannova J, Adamova E, Matalova E (2015) Pharmacological caspase inhibitors: research towards therapeutic perspectives. *J Physiol Pharmacol* 66(4):473–482
- Kumar AK, Zothantluanga JH, Aswin K, Maulana S, Sulaiman Zubair M, Lalhlenmawia H, Rudrapal M, Chetia D (2022) Antiviral phytocompounds “ellagic acid” and “(+)-sesamin” of *Bridelia Retusa* identified as potential inhibitors of SARS-COV-2 3CL pro using extensive molecular docking, molecular dynamics simulation studies, binding free energy calculations, and bioactivity prediction. *Struct Chem* 33:1445–1465. <https://doi.org/10.1007/s11224-022-01959-3>
- Kumar S, Bhardwaj VK, Singh R, Purohit R (2023) Structure restoration and aggregate inhibition of V30M mutant transthyretin protein by potential quinoline molecules. *Int J Biol Macromol* 231:123318. <https://doi.org/10.1016/j.ijbiomac.2023.123318>
- Kuribayashi K, Mayes PA, El-Deiry WS (2006) What are caspases 3 and 7 doing upstream of the mitochondria? *Cancer Biol Ther* 5(7):763–765. <https://doi.org/10.4161/cbt.5.7.3228>
- Lakhani SA, Masud A, Kuida K, Porter GA Jr, Booth CJ, Mehal WZ, Inayat I, Flavell RA (2006) Caspases 3 and 7: key mediators of mitochondrial events of apoptosis. *Science* 311(5762):847–851. <https://doi.org/10.1126/science.1115035>
- Laskowski RA, Gerick F, Thornton JM (2009) The structural basis of allosteric regulation in proteins. *FEBS Lett* 583(11):1692–1698. <https://doi.org/10.1016/j.febslet.2009.03.019>
- Lee D, Long SA, Adams JL, Chan G, Vaidya KS, Francis TA, Kikly K, Winkler JD, Sung CM, Debouck C, Richardson S, Levy MA, DeWolf WE Jr, Keller PM, Tomaszek T, Head MS, Ryan MD, Haltiwanger RC, Liang PH, Janson CA, McDevitt PJ, Johanson K, Concha NO, Chan W, Abdel-Meguid SS, Badger AM, Lark MW, Nadeau DP, Suva LJ, Gowen M, Nuttall ME (2000) Potent and selective nonpeptide inhibitors of caspases 3 and 7 inhibit apoptosis and maintain cell functionality. *J Biol Chem* 275(21):16007–16014. <https://doi.org/10.1074/jbc.275.21.16007>
- Lee D, Long SA, Murray JH, Adams JL, Nuttall ME, Nadeau DP, Kikly K, Winkler JD, Sung CM, Ryan MD, Levy MA, Keller PM, DeWolf WE Jr (2001) Potent and selective nonpeptide inhibitors of caspases 3 and 7. *J Med Chem* 44(12):2015–2026. <https://doi.org/10.1021/jm100537>
- Loftus LV, Amend SR, Pienta KJ (2022) Interplay between cell death and cell proliferation reveals new strategies for cancer therapy. *Int J Mol Sci* 23(9):4723. <https://doi.org/10.3390/ijms23094723>
- MacKenzie SH, Schipper JL, Clark AC (2010) The potential for caspases in drug discovery. *Curr Opin Drug Discov Devel* 13(5):568–576
- Minini L, Ferraro F, Cancela S, Merlino A (2017) Insight into the mechanism of action and selectivity of caspase-3 reversible inhibitors through in silico studies. *J Mol Struct* 1147:558–568. <https://doi.org/10.1016/j.molstruc.2017.06.118>
- Mohan A, Rendine N, Mohammed MK, Jeeva A, Ji H-F, Talluri VR (2021) Structure-based virtual screening, in silico docking, ADME Properties Prediction and molecular dynamics studies for the identification of potential inhibitors against SARS-COV-2 M^{pp}. *Mol Divers* 26:1645–1661. <https://doi.org/10.1007/s11030-021-10298-0>
- Murakami Y, Notomi S, Hisatomi T, Nakazawa T, Ishibashi T, Miller JW, Vavvas DG (2013) Photoreceptor cell death and rescue in retinal detachment and degenerations. *Prog Retin Eye Res* 37:114–140. <https://doi.org/10.1016/j.preteyeres.2013.08.001>
- Nile SH, Park SW (2014) Edible berries: bioactive components and their effect on human health. *Nutrition* 30(2):134–144. <https://doi.org/10.1016/j.nut.2013.04.007>
- O'Brien MA, Kirby R (2008) Apoptosis: a review of pro-apoptotic and anti-apoptotic pathways and dysregulation in disease. *J Vet Emerg Crit Care (San Antonio)* 18(6):572–585. <https://doi.org/10.1111/j.1476-4431.2008.00363.x>

- Ouyang L, Shi Z, Zhao S, Wang F-T, Zhou T-T, Liu B, Bao J-K (2012) Programmed cell death pathways in cancer: a review of apoptosis, autophagy and programmed necrosis. *Cell Prolif* 45(6):487–498. <https://doi.org/10.1111/j.1365-2184.2012.00845.x>
- Parrish AB, Freel CD, Kornbluth S (2013) Cellular mechanisms controlling caspase activation and function. *Cold Spring Harb Perspect Biol* 5:a008672. <https://doi.org/10.1101/cshperspect.a008672>
- Rahman MA, Hannan MA, Dash R, Rahman MH, Islam R, Uddin MJ, Sohag AAM, Rahman MH, Rhim H (2021) Phytochemicals as a complement to cancer chemotherapy: pharmacological modulation of the autophagy-apoptosis pathway. *Front Pharmacol* 12:639628. <https://doi.org/10.3389/fphar.2021.639628>
- Ramírez D, Caballero J (2018) Is it reliable to take the molecular docking top scoring position as the best solution without considering available structural data? *Molecules* 23(5):1038. <https://doi.org/10.3390/molecules23051038>
- Renis M, Calandra L, Scifo C, Tomasello B, Cardile V, Vanella L, Bei R, Fauci LL, Galvano F (2008) Response of cell cycle/stress-related protein expression and DNA damage upon treatment of caco2 cells with anthocyanins. *Br J Nutr* 100(1):27–35. <https://doi.org/10.1017/s0007114507876239>
- Seeram NP, Adams LS, Zhang Y, Lee R, Sand D, Scheuller HS, Heber D (2006) Blackberry, black raspberry, blueberry, cranberry, Red Raspberry, and strawberry extracts inhibit growth and stimulate apoptosis of human cancer cells in vitro. *J Agric Food Chem* 54(25):9329–9339. <https://doi.org/10.1021/jf061750g>
- Sepehri S, Razzaghi-Asl N, Mirzayi S, Mahnam K, Adhami V (2022) In silico screening and molecular dynamics simulations toward new human papillomavirus 16 type inhibitors. *Res Pharm Sci* 17(2):189–208. <https://doi.org/10.4103/1735-5362.335177>
- Sheikh SY, Ansari WA, Hassan F, Faruqui T, Khan MF, Akhter Y, Khan AR, Siddiqui MA, Al-Khedhairi AA, Nasibullah M (2023a) Drug repositioning to discover novel ornithine decarboxylase inhibitors against visceral leishmaniasis. *J Mol Recognit* 36:e3021. <https://doi.org/10.1002/jmr.3021>
- Sheikh SY, Ansari WA, Hassan F, Khan MF, Faiyaz SS, Akhter Y, Khan AR, Nasibullah M (2023b) Drug repurposing against phosphomannomutase for the treatment of cutaneous leishmaniasis. *Orient J Chem* 39(1):01–10. <https://doi.org/10.13005/ojc/390101>
- Shen SC, Chen YC, Hsu FL, Lee WR (2003) Differential apoptosis-inducing effect of quercetin and its glycosides in human promyeloleukemic HL-60 cells by alternative activation of the caspase 3 cascade. *J Cell Biochem* 89(5):1044–1055. <https://doi.org/10.1002/jcb.10559>
- Shi Y (2002) Mechanisms of caspase activation and inhibition during apoptosis. *Mol Cell* 9(3):459–470. [https://doi.org/10.1016/s1097-2765\(02\)00482-3](https://doi.org/10.1016/s1097-2765(02)00482-3)
- Shi JB, Tang WJ, Qi XB, Li R, Liu XH (2015) Novel pyrazole-5-carboxamide and pyrazole-pyrimidine derivatives: synthesis and anticancer activity. *Eur J Med Chem* 90:889–896. <https://doi.org/10.1016/j.ejmech.2014.12.013>
- Shimmyo Y, Kihara T, Akaike A, Niidome T, Sugimoto H (2008) Three distinct neuroprotective functions of myricetin against glutamate-induced neuronal cell death: involvement of direct inhibition of caspase-3. *J Neurosci Res* 86(8):1836–1845. <https://doi.org/10.1002/jnr.21629>
- Singh R, Purohit R (2023) Computational analysis of protein-ligand interaction by targeting a cell cycle restrainer. *Comput Methods Programs Biomed* 231:107367. <https://doi.org/10.1016/j.cmpb.2023.107367>
- Singh R, Manna S, Nandanwar H, Purohit R (2024) Bioactives from medicinal herb against bedaquiline resistant tuberculosis: removing the dark clouds from the horizon. *Microbes Infect* 26(3):105279. <https://doi.org/10.1016/j.micinf.2023.105279>
- Tallei TE, Tumilaar SG, Niode NJ, Fatimawali KBJ, Idroes R, Effendi Y, Sakib SA, Emran TB (2020) Potential of plant bioactive compounds as SARS-COV-2 main protease (M^{pro}) and spike (S) glycoprotein inhibitors: a molecular docking study. *Scientifica* 2020:1–18. <https://doi.org/10.1155/2020/6307457>
- Teli DM, Shah MB, Chhabria MT (2021) In silico screening of natural compounds as potential inhibitors of SARS-COV-2 main protease and Spike RBD: targets for covid-19. *Front Mol Biosci* 7:599079. <https://doi.org/10.3389/fmolb.2020.599079>
- Tuccinardi T (2021) What is the current value of MM/PBSA and MM/GBSA methods in drug discovery? *Expert Opin Drug Discov* 16(11):1233–1237. <https://doi.org/10.1080/17460441.2021.1942836>
- Wadegaonkar VP, Wadegaonkar PA (2012) Withaferin A targets apoptosis inhibitor cIAP1: a potential anticancer candidate. *J Appl Pharm Sci* 2(5):154–157
- Wadegaonkar VP, Wadegaonkar PA (2013) Withanone as an inhibitor of survivin: a potential drug candidate for cancer therapy. *J Biotechnol* 168(2):229–233. <https://doi.org/10.1016/j.jbiotec.2013.08.028>
- Wang IK, Lin-Shiau SY, Lin JK (1999) Induction of apoptosis by apigenin and related flavonoids through cytochrome *c* release and activation of caspase-9 and caspase-3 in leukaemia HL-60 cells. *Eur J Cancer* 35(10):1517–1525
- Xu G, Shi Y (2007) Apoptosis signaling pathways and lymphocyte homeostasis. *Cell Res* 17:759–771. <https://doi.org/10.1038/cr.2007.52>
- Zhao C, Giusti MM, Malik M, Moyer MP, Magnuson BA (2004) Effects of commercial anthocyanin-rich extracts on colonic cancer and nontumorigenic colonic cell growth. *J Agric Food Chem* 52(20):6122–6128. <https://doi.org/10.1021/jf049517a>

Springer Nature or its licensor (e.g. a society or other partner) holds exclusive rights to this article under a publishing agreement with the author(s) or other rightsholder(s); author self-archiving of the accepted manuscript version of this article is solely governed by the terms of such publishing agreement and applicable law.